Intramolecular Photochemical Electron Transfer. 4. Singlet and Triplet Mechanisms of Electron Transfer in a Covalently Linked Porphyrin-Amide-Quinone Molecule†

John A. Schmidt,‡ Alan R. McIntosh,‡ Alan C. Weedon,*‡ James R. Bolton,*‡ John S. Connolly,*§ John K. Hurley,§ and Michael R. Wasielewski*⊥

Contribution from the Photochemistry Unit, Department of Chemistry, The University of Western Ontario, London, Ontario, Canada N6A 5B7, Photoconversion Research Branch, Solar Energy Research Institute, 1617 Cole Boulevard, Golden, Colorado 80401, and Chemistry Division, Argonne National Laboratory, Argonne, Illinois 60439. *Received July 22, 1987*

Abstract: We have carried out an extensive photophysical analysis of a tetraarylporphine linked through a single amide bridge to either methyl-*p*-benzoquinone (PAQ) or the corresponding hydroquinone ($PAQH_2$) in benzonitrile as the solvent. The photophysical properties of $PAQH_2$ are closely similar to those of nonlinked tetraarylporphine species, while for PAQ significant lifetime quenching of both the lowest excited singlet and triplet states is observed. Picosecond transient absorption spectroscopy and fluorescence lifetime measurements were used to show that quenching of the excited singlet state of PAQ is due to intramolecular electron transfer to the singlet radical ion pair $^1(P^{\bullet+}AQ^{\bullet-})$ with a rate constant of 4.1 (±0.3) × 10^8 s^{-1}. $^1(P^{\bullet+}AQ^{\bullet-})$ subsequently decays to the ground state by reverse electron transfer with a rate constant of 1.6 (±0.2) × 10^8 s^{-1}. This reaction has $\Delta G^\circ \cong -1.4$ eV and is predicted to be in the Marcus inverted region. The experimental ratio of the forward to reverse rate constants is very similar to that predicted by Marcus theory. Nanosecond flash photolysis studies show that the lowest triplet state of PAQ is also quenched, most likely by electron transfer to the triplet radical ion pair $^3(P^{\bullet+}AQ^{\bullet-})$, with a rate constant of 4.6 (±0.2) × 10^4 s^{-1}. We suggest that $^3(P^{\bullet+}AQ^{\bullet-})$ interconverts rapidly with $^1(P^{\bullet+}AQ^{\bullet-})$, which then decays rapidly to the ground state.

Covalently linked porphyrin-quinone compounds are important as models of the light-induced electron transfer that occurs in photosynthetic reaction centers. Strategies used for linking the donor and acceptor include diester- and diamide-linked polymethylene chains,[1,2] rigid triptycenyl[3] and bicyclo[2.2.2]octyl[4] spacers, "capped"[5] structures, and molecules that include secondary electron donors[6] or acceptors.[7] In some cases, nitrobenzenes,[8] methyl viologen,[9] or pyromellitic anhydride[10] have been used as electron acceptors. The importance of eliminating diffusion effects in studies of electron-transfer reactions has been elegantly argued by Miller et al.[11] and has been highlighted by the recent observation of the elusive Marcus "inverted" region[12] in three different intramolecular systems.[3a,5c,14]

Previously, we reported[15] the solvent dependence of the rate of electron-transfer quenching of the excited singlet state of a covalently linked porphyrin-amide-*p*-benzoquinone (PAQ, I). These data suggested that benzonitrile is a particularly favorable solvent in which to achieve a high quantum yield of charge separation in PAQ.

In this paper we analyze more closely the photophysical behavior of these molecules in benzonitrile and provide evidence for the formation of the radical ion pair $P^{\bullet+}AQ^{\bullet-}$ by two distinct routes. First, oxidation of the lowest excited singlet state (S_1) of the porphyrin by the attached quinone yields the singlet radical ion pair $^1(P^{\bullet+}AQ^{\bullet-})$. Second, we also have evidence that the lowest triplet state (T_1) of P is oxidized by the quinone to form the triplet radical ion pair $^3(P^{\bullet+}AQ^{\bullet-})$.

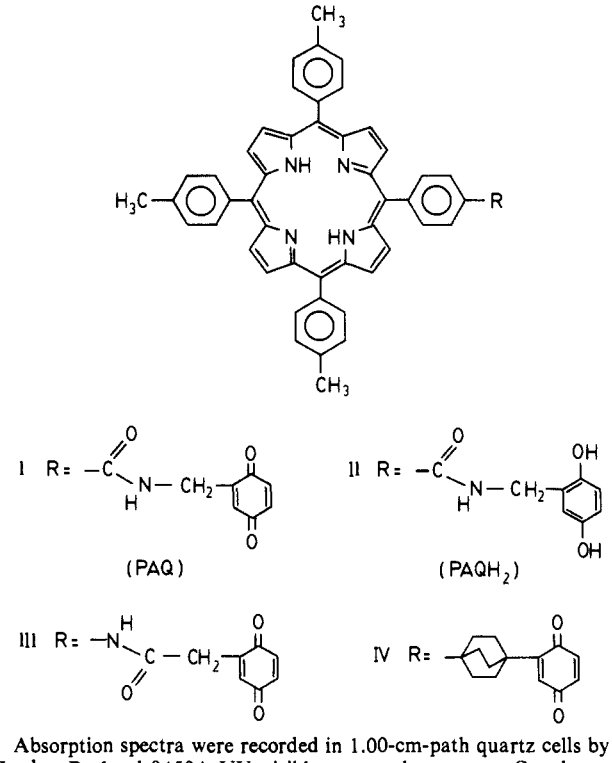

Experimental Section

The synthesis and characterization of PAQ and its hydroquinone derivative $PAQH_2$ (II) have been described previously.[15,16] The material was stored as $PAQH_2$; samples of PAQ were freshly prepared before each experiment by oxidation of $PAQH_2$ with PbO_2 in a CH_2Cl_2 solution.[2a] After 10-15 min of agitation, the lead residues were removed with a 10-μm Millipore filter; the success of the oxidation was confirmed by the appearance of a characteristic quinone absorption band at 246 nm.[2a,c] The solvent was then evaporated in a stream of dry nitrogen, and the PAQ residue was taken up in HPLC-grade benzonitrile (Aldrich).

Absorption spectra were recorded in 1.00-cm-path quartz cells by a Hewlett-Packard 8450A UV-visible spectrophotometer. Steady-state

† Contribution No. 381 from the Photochemistry Unit, The University of Western Ontario.

‡ The University of Western Ontario.

§ Solar Energy Research Institute.

⊥ Argonne National Laboratory.

(1) (a) Kong, J. L. Y.; Loach, P. A. *J. Heterocycl. Chem.* **1980**, *17*, 737-744. (b) Kong, J. L. Y.; Spears, K. G.; Loach, P. A. *Photochem. Photobiol.* **1982**, *35*, 545-553. (c) Ho, T.-F.; McIntosh, A. R.; Bolton, J. R. *Nature (London)* **1980**, *286*, 254-256.

(2) (a) Paper 1: McIntosh, A. R.; Siemiarczuk, A.; Bolton, J. R.; Stillman, M. J.; Ho, T.-F.; Weedon, A. C. *J. Am. Chem. Soc.* **1983**, *105*, 7215-7223. (b) Paper 2: Siemiarczuk, A.; McIntosh, A. R.; Ho, T.-F.; Stillman, M. J.; Roach, K. J.; Weedon, A. C.; Bolton, J. R.; Connolly, J. S. *J. Am. Chem. Soc.* **1983**, *105*, 7224-7230. (c) Ho, T.-F.; McIntosh, A. R.; Weedon, A. C. *Can. J. Chem.* **1984**, *62*, 967-974.

(3) (a) Wasielewski, M. R.; Niemczyk, M. P.; Svec, W. A.; Pewitt, E. B. *J. Am. Chem. Soc.* **1985**, *107*, 1080-1082. (b) Wasielewski, M. R.; Niemczyk, M. P. *J. Am. Chem. Soc.* **1984**, *106*, 5043-5045. (c) Wasielewski, M. R.; Niemczyk, M. P. *ACS Symp. Ser.* **1986**, *321*, 154-165.

0002-7863/88/1510-1733$01.50/0

fluorescence spectra were recorded with samples in 1.00 × 1.00 cm quartz cells in a Perkin-Elmer 650-40 spectrofluorometer. Fluorescence quantum yields ϕ_f in benzonitrile were estimated by comparing emission intensities integrated between 620 and 750 nm with that of 5-(4-carboxyphenyl)-10,15,20-tri-*p*-tolylporphine[2c] (TTPa) for which ϕ_f is 0.11,[17] measured relative to *meso*-tetraphenylporphine (TPP) in benzene (ϕ_f = 0.13) as a secondary standard.[18]

Fluorescence lifetimes τ_f were determined as previously described[2b] by the method of time-correlated single-photon counting with a PRA International Model 3000 nanosecond lifetime fluorometer, with a PRA International Model 510 hydrogen flash lamp (~2-ns fwhm) as the excitation source.

Picosecond time-resolved transient absorption measurements were obtained at Argonne in the following manner: 2.0×10^{-4} M solutions of PAQ were prepared in benzonitrile as outlined above and placed in 2-mm path length cuvettes. The samples were deoxygenated by purging ~30 min with dry, prepurified nitrogen. The output of a mode-locked argon ion laser synchronously pumped rhodamine-6G dye laser (610 nm, ~1.5-ps pulse duration, and ~1.0-nJ energy) was amplified to 2.5 mJ by a four-stage, rhodamine-640 dye amplifier. Each stage of the amplifier was pumped longitudinally by a frequency-doubled Nd-YAG laser operating at 10 Hz. The amplified 610-nm laser pulse was split with a dichroic mirror. A ~1.5-ps, ~2.0-mJ pulse was used to generate a ~1.5-ps white-light continuum probe pulse. The remaining ~0.5 mJ of 610-nm light was used to excite the sample.

Absorbance measurements were made with a double-beam probe configuration, which employed optical multichannel detection. A 2-mm-diameter spot on the sample cell was illuminated with both the pump and probe beams, while a different 2-mm spot on the sample was illuminated only with the reference probe beam. The reference and measuring beams were each imaged onto half of the input slit of an ISA HR-320 monochromator. The two dispersed spectra were recorded with a PAR OMA II 1254E intensified vidicon detector/1216 controller and transferred to a DEC 11/73 computer system for computation of the absorbance changes ΔA and kinetics and for storage and display of the data. Time delays (±20 ps) between arrival of the pump and probe pulses at the sample were accomplished with a computer-controlled optical delay line. Kinetic analyses of the data were carried out by the method of Provencher.[19]

Nanosecond flash photolysis experiments were conducted with two different sets of apparatus, one at The University of Western Ontario (UWO) and the other at the Solar Energy Research Institute (SERI). The UWO setup consisted of a PRA International Model LN-1000 pulsed nitrogen laser (337-nm, ~0.5-mJ, ~0.8-ns fwhm pulses), a tungsten–halogen monitoring lamp (focused onto sample entrance slits, each with a 1.3-mm aperture on a 1.0-cm path collinear with the excitation path), a Jarrell-Ash 0.25-m monochromator, and a Hamamatsu R-928 photomultiplier tube. The signals were digitized by a Nicolet Explorer 2090-III transient recorder (time resolution of ~100 ns) coupled to a Nicolet 1180 computer.

The temporal profiles of the absorbance changes at the wavelengths of interest were determined by averaging the signals induced by 256 laser pulses. Experiments were always carried out in parallel on samples of PAQ and $PAQH_2$, each with the same absorbance at the excitation wavelength. Samples were deoxygenated by purging with nitrogen gas for ~30 min before starting an experiment and were continuously purged while flashing. The virtue of this system was that the low excitation energy incident on a small sample aliquot (~0.05 cm^3) minimized photoreduction of PAQ, and a single sample could receive over 2×10^4 0.5-mJ flashes at 337 nm with no significant change in composition. The signal-to-noise ratios of the data obtained at UWO were lower than those obtained at SERI primarily because of the low pulse energy of the nitrogen laser. However, it was still possible to analyze the kinetics out to 800 nm where $\Delta A \cong 0.02$.

The system at SERI utilized the second harmonic (532 nm) of a Molectron MY35 Nd:YAG laser (20-ns fwhm) for excitation. The monitoring beam (450-W Xenon lamp) was perpendicular to the excitation beam and was passed through a Spex Minimate monochromator positioned before the sample and through a Spex Doublemate monochromator placed after the sample. The signals, derived from 4–16 repetitive laser pulses, were detected by a Hamamatsu R928 photomultiplier tube (truncated at the fifth dynode), amplified by a Pacific Instruments Model 2A50 wide-band (dc to 240 MHz) amplifier and digitized by a Tektronix 7912AD transient recorder. The bandwidth limit of this system is ~5 ns (200 MHz), and reproducible absorbance changes ($\geq 4 \times 10^{-4}$) can be detected under the stated conditions. A DEC PDP 11/34A computer was used for data acquisition, storage, and analysis and for control of various components (shutters, monochromators, laser Q-switch trigger). A complete description will appear elsewhere.[20]

The relatively high pulse energies of the excitation source (≥80 mJ/pulse) and high irradiance of the monitoring beam (~10 W m^{-2} at 450 nm) resulted in traces with peak signal-to-noise ratios of ~200:1, so that kinetic analyses could be carried out even on the weak triplet absorptions observed in the red (600–830 nm).[21] In addition, the beam geometry in this system produces a uniform concentration of porphyrin triplet states, so that complex decay kinetics can be analyzed reliably. A drawback of the high excitation energy and monitoring irradiance and large irradiated sample aliquot (~1 cm^3) was that measurable photoreduction of PAQ to $PAQH_2$ occurred during a typical run (4–16 pulses at each of 10–20 different wavelengths). The extent of photoreduction was monitored by periodically examining the initial absorbance changes ΔA_0 at ~0.98 μs after the laser pulse at some reference wavelength (usually 450 nm). An increased value of ΔA_0 during a run indicated that some $PAQH_2$ had been produced, since this species has a higher triplet yield than PAQ. The relative amounts of PAQ and $PAQH_2$ could also be determined from the fluorescence decay profiles, as described below.

The decay kinetics of the triplet state of $PAQH_2$ ($^3PAQH_2$) were obtained from a sample that was degassed by 6–8 freeze–pump–thaw cycles in a side arm attached to a 1.00 × 1.00-cm quartz fluorescence cell. The assembly was then sealed off at a pressure of $\leq 7 \times 10^{-5}$ Pa. This procedure precluded oxygen quenching of the long-lived porphyrin triplet state. A concentrated sample (2×10^{-5} M) was used to obtain

(4) (a) Joran, A. D.; Leland, B. A.; Geller, G. G.; Hopfield, J. J.; Dervan, P. B. *J. Am. Chem. Soc.* **1984**, *106*, 6090–6092. (b) Leland, B. A.; Joran, A. D.; Felker, P. M.; Hopfield, J. J.; Zewail, A. H.; Dervan, P. B. *J. Phys. Chem.* **1985**, *89*, 5571–5573. (c) Bolton, J. R.; Ho, T.-F.; Liauw, S.; Siemiarczuk, A.; Wan, C. S. K.; Weedon, A. C. *J. Chem. Soc., Chem. Commun.* **1985**, 559–560.

(5) (a) Lindsey, J. S.; Mauzerall, D. C.; Linschitz, H. *J. Am. Chem. Soc.* **1983**, *105*, 6528–6529. (b) Ganesh, K. N.; Sanders, J. K. M. *J. Chem. Soc., Perkin Trans. 1* **1982**, 1611–1615. (c) Irvine, M. P.; Harrison, R. J.; Beddard, G. S.; Leighton, P.; Sanders, J. K. M. *Chem. Phys.* **1986**, *104*, 315–324.

(6) (a) Wasielewski, M. R.; Niemczyk, M. P.; Svec, W. A.; Pewitt, E. B. *J. Am. Chem. Soc.* **1985**, *107*, 5562–5563. (b) Moore, T. A.; Gust, D.; Mathis, P.; Mialocq, J.-C.; Chachaty, C.; Bensasson, R. V.; Land, E. J.; Doizi, D.; Liddell, P. A.; Lehman, W. R.; Nemeth, G. A.; Moore, A. L. *Nature (London)* **1984**, *307*, 630–632.

(7) Nishitani, S.; Kurata, N.; Sakata, Y.; Misumi, S.; Karen, A.; Okada, T.; Mataga, N. *J. Am. Chem. Soc.* **1983**, *105*, 7771–7772.

(8) (a) Maiya, G. B.; Krishnan, V. *J. Phys. Chem.* **1985**, *89*, 5225–5235. (b) Krüger, H. W.; Koehorst, R. B. M.; van Hoek, A.; Schaafsma, T. J.; Michel-Beyerle, M. E. In *Advances in Photosynthesis Research*; Sybesma, C., Ed.; Nijhoff/Junk Publishers: The Hague/Boston/Lancaster, 1984; Vol. 1, pp 721–724.

(9) (a) Harriman, A.; Porter, G.; Wilowska, A. *J. Chem. Soc., Faraday Trans. 2* **1984**, *80*, 191–204. (b) Leighton, P.; Sanders, J. K. M. *J. Chem. Soc., Chem. Commun.* **1984**, 856–857. (c) Blondeel, G.; De Keukeleire, D.; Harriman, A.; Milgrom, L. R. *Chem. Phys. Lett.* **1985**, *118*, 77–82.

(10) (a) Cowan, J. A.; Sanders, J. K. M. *J. Chem. Soc., Perkin Trans 1* **1985**, 2435–2437. (b) Cowan, J. A.; Sanders, J. K. M.; Beddard, G. S.; Harrison, R. J. *J. Chem. Soc., Chem. Commun.* **1987**, 55–58.

(11) Miller, J. R.; Beitz, J. V.; Huddleston, R. K. *J. Am. Chem. Soc.* **1984**, *106*, 5057–5068.

(12) The Marcus theory[13] predicts that the rate of an outer-sphere electron transfer is a quadratic function of the reaction Gibbs energy. Thus, the rate should increase with increasing exergonicity to some maximum, which is characteristic of the system, and then decrease with further increases in exergonicity. The latter condition defines the "inverted" region.

(13) (a) Marcus, R. A. *J. Chem. Phys.* **1956**, *24*, 966–978. (b) Marcus, R. A. *Annu. Rev. Phys. Chem.* **1964**, *15*, 155–196. (c) Marcus, R. A.; Sutin, N. *Biochim. Biophys. Acta* **1985**, *811*, 265–322. (d) Newton, M. D.; Sutin, N. *Annu. Rev. Phys. Chem.* **1984**, *35*, 437–480.

(14) Miller, J. R.; Calcaterra, L. T.; Closs, G. L. *J. Am. Chem. Soc.* **1984**, *106*, 3047–3049.

(15) Paper 3: Schmidt, J. A.; Siemiarczuk, A.; Weedon, A. C.; Bolton, J. R. *J. Am. Chem. Soc.* **1985**, *107*, 6112–6114.

(16) Schmidt, J. A. Ph.D. Thesis, The University of Western Ontario, London, Canada, 1986.

(17) Hurley, J. K.; Marsh, K. L.; Bell, W. L.; Wasielewski, M. R.; Connolly, J. S., to be submitted for publication.

(18) (a) Quimby, D. J.; Longo, F. R. *J. Am. Chem. Soc.* **1975**, *97*, 5111–5117. (b) Seybold, P. G.; Gouterman, M. *J. Mol. Spectrosc.* **1969**, *31*, 1–13.

(19) Provencher, S. W. *J. Chem. Phys.* **1976**, *64*, 2772.

(20) Connolly, J. S.; Marsh, K. L.; Cook, D. R.; Bolton, J. R.; McIntosh, A. R.; Weedon, A. C.; Ho, T.-F., to be submitted for publication.

(21) (a) McIntosh, A. R.; Bolton, J. R.; Connolly, J. S.; Marsh, K. L.; Cook, D. R.; Ho, T.-F.; Weedon, A. C. *J. Phys. Chem.* **1986**, *90*, 5640–5646. (b) Connolly, J. S.; Marsh, K. L.; Cook, D. R.; Bolton, J. R.; McIntosh, A. R.; Siemiarczuk, A.; Weedon, A. C.; Ho, T.-F. *Sci. Pap. Inst. Phys. Chem. Res. (Jpn).* **1984**, *78*, 118–128.

Table I. Photophysical Parameters for TTPm, TTPa, $PAQH_2$, and PAQ in Benzonitrile at Room Temperature

	τ_f[a]/ns	ϕ_f	$k_F/10^7\ s^{-1}$	ϕ_{isc}	$k_{isc}/10^7\ s^{-1}$	ϕ_{ic}[b]	k_{ic}[b]$/10^7\ s^{-1}$	$k_{et}^S/10^8\ s^{-1}$	ϕ_{et}
TTPm[c]	11.6_0	0.11_1[d]	0.95_7	0.67[e]	5.8	0.22	1.9		
TTPa[f]	11.3_6	0.10_8[d]	0.95_1	0.67[g]	5.9	0.22	1.9		
$PAQH_2$	11.7_0	0.12_5	1.07	0.67[g]	5.7	0.20	1.8		
PAQ	2.0_1	0.025	1.24	0.11_5	5.7[h]	0.03_2	1.8	4.1[i]	0.82_8

[a] ±5%. [b] By difference; ±15%. [c] 5-(4-Carbomethoxyphenyl)-10,15,20-tri-*p*-tolylporphine. [d] Measured[17] relative to $\phi_f = 0.13$ for TPP in benzene.[18] [e] Calculated from $\phi_{isc}E_T = 0.96 \pm 0.03$ eV[29] for TTP with $E_T = 1.43 \pm 0.01$ eV.[22b] [f] 5-(4-Carboxyphenyl)-10,15,20-tri-*p*-tolylporphine. [g] Assumed to be the same as TTPm and TTP (see text). [h] Assumed to be the same as $PAQH_2$. [i] ±8%.

spectral and kinetic data at long wavelengths (500–830 nm). From 300 to 500 nm, where the porphyrin ground-state absorption is more intense, the sample was diluted by distilling solvent from the side arm into the cell.

The transient absorption observed in PAQ decays much faster than that in $PAQH_2$, and the kinetics observed are essentially independent of whether the sample was deoxygenated by nitrogen or argon bubbling or by vacuum-line degassing. We also noted that in some cases the freeze–pump–thaw regimen itself resulted in significant reduction of the quinone to the hydroquinone, even under very dim light. Accordingly, the data reported here for PAQ were taken on samples that were purged with nitrogen gas in situ in a long-stem fluorescence cuvette fitted with a rubber septum.

Results and Discussion

1. Absorption and Fluorescence Spectra. The absorption spectrum of PAQ is identical with that of a solution that is equimolar in the *n*-propylamide of 5-(4-carboxyphenyl)-10,15,20-tri-*p*-tolylporphine and the *n*-propylamide of (1,4-benzoquinonyl)acetic acid. There is no broadening or red-shifting of either the porphyrin absorption or emission bands, such as that found[2b] for porphyrin–quinone molecules with an amide–polymethylene–amide linkage. These observations provide good evidence for the absence of ground-state interactions between the porphyrin ring and its attached quinone. These comments also apply to $PAQH_2$.

2. Energetics. The energies of the various states of PAQ relative to the ground state are shown in Figure 1. The first excited singlet state of PAQ ($^1P^*AQ$) lies at about 1.90 (±0.01) eV, as determined from the overlap of the normalized absorption and emission spectra. The energy of the triplet state of TPP is about 1.43 eV at 77 K.[22] The energy of the charge-separated radical-ion-pair state ($P^{\bullet+}AQ^{\bullet-}$) has been estimated from redox potentials determined by differential pulse voltammetry[23] to be ~1.41 eV in benzonitrile, which includes a small correction (−0.04 eV) for coulombic stabilization of two charges at a distance of 14 Å (see below). Assuming that the standard entropy change between the ground state and first excited singlet state is negligible and that further stabilization of $P^{\bullet+}AQ^{\bullet-}$ relative to $P^{\bullet+}AQ$ and $PAQ^{\bullet-}$ by spin–spin interactions is small, the standard Gibbs energy change $\Delta G_{et}°$ in PAQ for electron transfer from the lowest excited singlet state to the attached quinone is exergonic by ~0.49 and ~0.02 eV from the lowest triplet state. Electrochemical measurements[23] of $\Delta G_{et}°$ for PAQ in a variety of solvents show that the energetics are strongly solvent dependent.

3. Excited Singlet-State Photophysics and Photochemistry. $^1P^*AQ$ can decay by fluorescence, internal conversion, or intersystem crossing to ^3PAQ or by electron transfer to the attached quinone, with respective rate constants k_f, k_{ic}, k_{isc}, and k_{et}^S. Values for these rate constants were obtained as described below from the measured fluorescence lifetimes τ_f of both PAQ and $PAQH_2$ (Table I).

At room temperature the fluorescence decay of $^1P^*AQH_2$ is completely described by a single exponential component with a lifetime in benzonitrile of 11.70 ± 0.05 ns.[15,16] In contrast, the decay of PAQ is biphasic, with lifetimes of 2.01 ± 0.02 (96%) and 11.2 ± 0.9 (4%) ns. The short-lived component is ascribed to the decay of $^1P^*AQ$, while the long-lived component probably arises from fluorescence of residual amounts of unoxidized

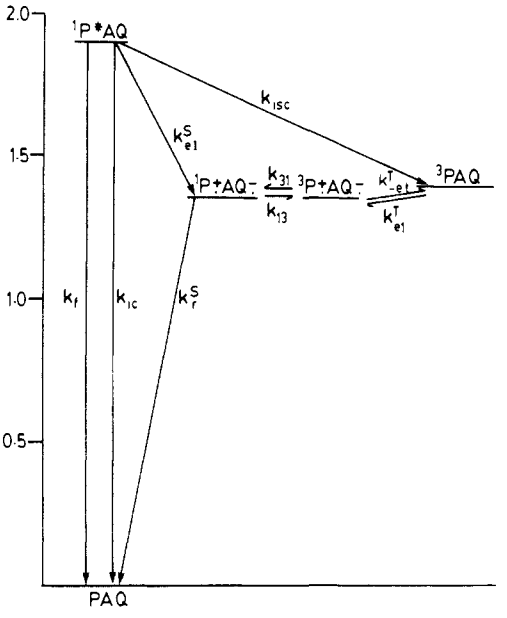

Figure 1. Energy level diagram for PAQ photophysics in benzonitrile. k_r^S is the back-electron-transfer rate from the singlet radical ion pair, and k_{31} is the rate constant for conversion from the $^3(P^{\bullet+}AQ^{\bullet-})$ state to the $^1(P^{\bullet+}AQ^{\bullet-})$ state by electron spin rephasing. The other rate constants are defined in the text.

$PAQH_2$. Small amounts of long-lived porphyrin fluorescence have been observed in several other porphyrin–quinone compounds and have been accounted for in the same way.[2,4b,5c] The preexponential factors indicate that freshly oxidized samples contain <5% $PAQH_2$. Examination of the preexponential factors provides a convenient monitor of the integrity of the quinone during laser flash photolysis of PAQ (see the Experimental Section). The radiative rate constant k_f is then given by $k_f = \phi_f/\tau_f$.

k_f, k_{ic}, and k_{isc} are properties of the porphyrin moiety; it is thus reasonable to assume that they do not change their values significantly when $PAQH_2$ is oxidized to PAQ. With the assumption that the shorter fluorescence lifetime of PAQ, relative to that of $PAQH_2$, is due entirely to electron transfer, the rate constant k_{et}^S for electron transfer from $^1P^*AQ$ is given by[2b] eq 1, where τ_1 and

$$k_{et}^S = 1/\tau_1 - 1/\tau_2 \quad (1)$$

τ_2 are the lifetimes of PAQ and $PAQH_2$, respectively. Using eq 1 and the lifetimes given above, we find $k_{et}^S = 4.1\ (\pm 0.3) \times 10^8\ s^{-1}$ in benzonitrile.

Transient absorption spectra of $PAQH_2$ and PAQ in benzonitrile at 100 ps and 6 ns following a 1.5-ps, 610-nm laser flash are shown in parts a and b of Figure 2, respectively. The traces obtained for these compounds at 100 ps are the S_1–S_0 difference spectra and are characterized by strong bleaching of the porphyrin bands at 510 and 650 nm and strong positive absorbance changes at all other wavelengths between 420 and 700 nm. The intensity of the positive absorbance changes decreases rapidly in the near-infrared. Similar spectral features between 550 and 750 nm have been observed previously for the lowest excited singlet state of TPP in CH_2Cl_2.[24]

(22) (a) Gouterman, M.; Khalil, G.-E. *J. Mol. Spectrosc.* **1974**, *53*, 88. (b) Harriman, A. *J. Chem. Soc., Faraday Trans. 1* **1980**, *76*, 1978–1985.
(23) Archer, M. D.; Gadzekpo, V. P. Y.; Bolton, J. R.; Schmidt, J. A.; Weedon, A. C. *J. Chem. Soc., Faraday Trans. 2* **1986**, *82*, 2305–2313.
(24) Bergkamp, M. A.; Dalton, J.; Netzel, T. L. *J. Am. Chem. Soc.* **1982**, *104*, 253–259.

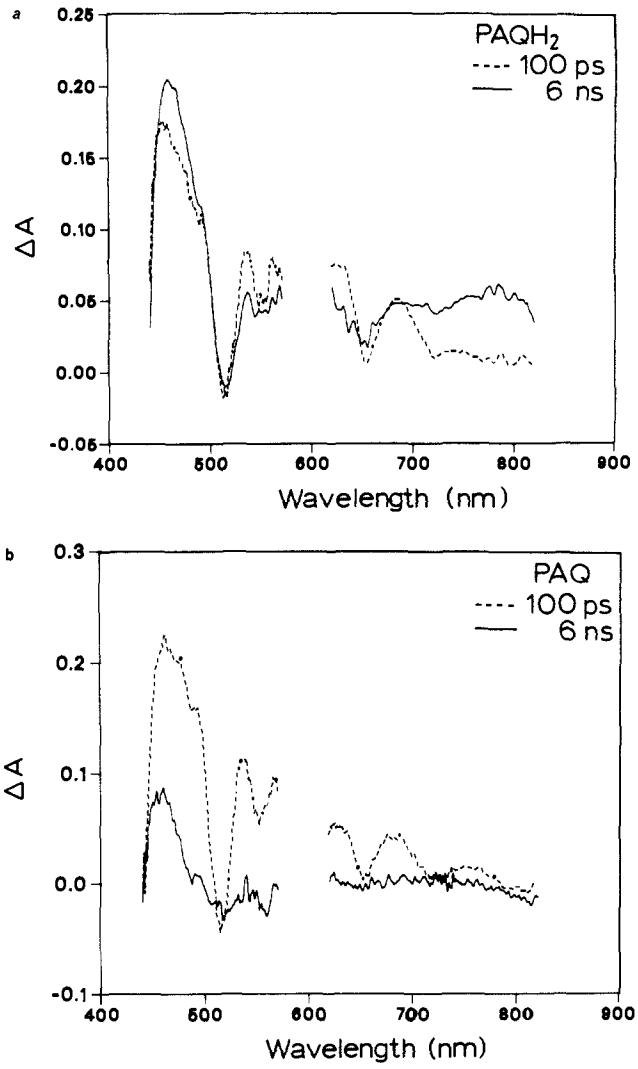

Figure 2. Transient absorption spectra in benzonitrile following a 1.5-ps, 610-nm laser flash. (a) $PAQH_2$: ---, 100 ps; —, 6 ns. (b) PAQ: ---, 100 ps; —, 6 ns. Wavelengths from 570 to 620 nm were blocked by filters used to reject residual 610-nm light from the continuum generation. Data at wavelengths shorter than 440 nm were not measured because the Soret band of the porphyrin strongly attenuates the probe light. (Data obtained at Argonne.)

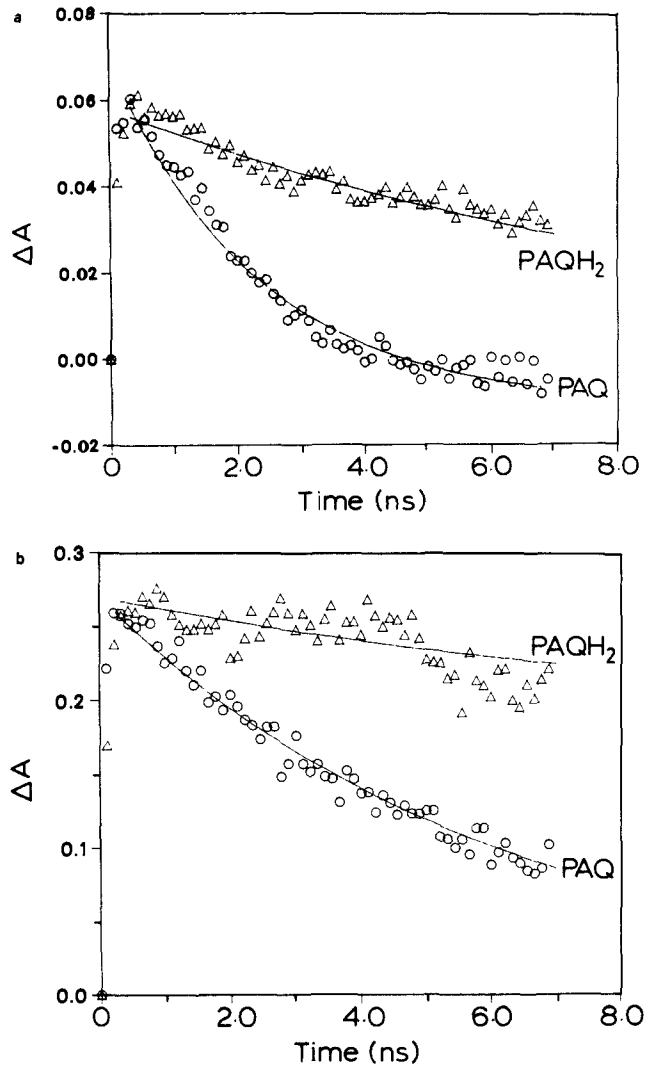

Figure 3. Transient absorption changes following a 1.5-ps, 610-nm laser flash. (a) 630 nm: △, $PAQH_2$; ○, PAQ. (b) 460 nm: △, $PAQH_2$; ○, PAQ. The solid curves are the exponential fits to the data. (Data obtained at Argonne.)

The spectral changes obtained 6 ns after the laser flash for $PAQH_2$ are characterized by a strong absorption feature centered at 470 nm and a broad absorbance near 790 nm. These spectral changes are indicative of $^3PAQH_2$ formation.[25] In contrast, the transient absorption spectrum of PAQ at 6 ns shows an absorption band at 460 nm that is less intense than that of $^1P^*AQ$ together with a broad absorption band near 720 nm. These spectral changes are very similar to those obtained on oxidation of *meso*-tetraarylporphines to their corresponding cation radicals.[26] Thus, the difference spectrum obtained 6 ns after laser excitation of PAQ is consistent with the formation of $P^{\bullet+}AQ^{\bullet-}$. The extinction coefficients of $Q^{\bullet-}$ are quite small in the wavelength band examined, and hence absorption by $Q^{\bullet-}$ does not contribute significantly to the difference spectra.

The differences in absorbance changes between $^1P^*AQH_2$ and $^3PAQH_2$ shown in Figure 2a and those between $^1P^*AQ$ and $P^{\bullet+}AQ^{\bullet-}$ shown in Figure 2b are significant at a number of wavelengths throughout each spectrum. The decay of the lowest excited singlet states (S_1) of the porphyrins in $^1P^*AQH_2$ and in $^1P^*AQ$ can be conveniently monitored at 630 nm where $P^{\bullet+}AQ^{\bullet-}$ does not absorb significantly. These data are illustrated in Figure 3a along with an exponential fit to the experimental points.

$^1P^*AQH_2$ and $^1P^*AQ$ each exhibit single exponential decay times of 10.5 ± 0.4 and 2.0 ± 0.2 ns, respectively, in good agreement with the S_1 lifetimes obtained from the time-resolved fluorescence measurements (Table I). The S_1 lifetimes of both $PAQH_2$ and PAQ show no important variations as a function of wavelength throughout the spectral region examined.

The decay of $P^{\bullet+}AQ^{\bullet-}$ is best followed by observing the absorbance change at 460 nm. The time dependence of this change is shown in Figure 3b along with the transient absorption changes for $PAQH_2$ at 460 nm. The data for PAQ can best be described by a sum of two exponential decays with a 2.0 (±0.2) ns (28%) component and a 6.1 (±0.2) ns (72%) component. The short-lived component is assigned to decay of $^1P^*AQ$, which also absorbs at 460 nm. The longer lived component is attributed to decay of $P^{\bullet+}AQ^{\bullet-}$ to the ground state. The spectral data in the 750–800-nm region show that there is no significant population of ^3PAQ via decay of $P^{\bullet+}AQ^{\bullet-}$. It should be noted that, because of low signal-to-noise ratios, triplet yields less than ~10% would not be detected.

The changes at 460 nm for $PAQH_2$ can be described by the sum of two single exponentials, one decreasing and one increasing, both with 10.5 ± 0.4 ns time constants but with relative amplitudes of 0.56 and 0.44, respectively; this is simply the decay of $^1P^*AQH_2$ and the formation of $^3PAQH_2$.

(25) Pekkarinen, L.; Linschitz, H. *J. Am. Chem. Soc.* **1960**, *82*, 2407–2411.
(26) Gasyna, Z.; Browett, W. R.; Stillman, M. J. *Inorg. Chem.* **1985**, *24*, 2440–2447.

To complete the description of excited singlet decay in $PAQH_2$, we have estimated the quantum yields of intersystem crossing ϕ_{isc} and internal conversion ϕ_{ic} from published values for unlinked tetraarylporphines. The importance of internal conversion to the decay of porphyrin excited singlet states is somewhat unclear. For TPP it has been widely assumed that $\phi_f + \phi_{isc} \cong 1$; i.e., internal conversion is negligible.[27] This is based on measurements of $\phi_f = 0.13$[18,28] and $\phi_{isc} = 0.82$–0.85.[27] More recently, Moore et al.,[29] using a photoacoustic technique, found that $\phi_{isc}E_T \approx 0.96$ eV for tetra-*p*-tolylporphine (TTP), where E_T is the energy of the lowest triplet state. Values of $\phi_{isc} > 0.8$ are inconsistent with this result, since they require E_T to be <1.2 eV. If we use a triplet energy of 1.43 eV,[22b] then $\phi_{isc} = 0.67$. Since $\phi_f = 0.11$, this requires that internal conversion be appreciable: i.e., $\phi_{ic} \cong 0.22$ (Table I). Studies of ZnTPP[30] and chlorophyll *a*[31] have shown that internal conversion cannot be neglected, contrary to earlier assertions.[27] Non-heavy-atom parasubstituents, which are neither strongly electron-withdrawing nor electron-donating, are not expected to induce significant perturbations in the emission characteristics of tetraarylporphines;[32] we therefore assume $\phi_{isc} \cong 0.67$ for $PAQH_2$. With our measured values of ϕ_f (0.12_5) and τ_f (11.7_0 ns) for $PAQH_2$, we estimate $\phi_{ic} \cong 0.20_4$, and therefore $k_{ic} \cong 1.7_5 \times 10^7$ s^{-1} and $k_{isc} \cong 5.7_3 \times 10^7$ s^{-1}. As mentioned above, oxidation of the hydroquinone end group to the quinone is not expected to affect the photophysical properties of the porphyrin ring, so it is reasonable to assume that k_{ic} and k_{isc} are essentially the same for PAQ and $PAQH_2$. For both molecules, k_f can be calculated from ϕ_f for $PAQH_2$, so that k_{ic} and ϕ_{ic} can be calculated by difference. Thus, all of the photophysical parameters for PAQ and $PAQH_2$ and the reference compounds, TTPm and TTPa, can be evaluated and are listed in Table I.

The S_1 state of the porphyrin in PAQ (I) is quenched by the attached quinone but not by the hydroquinone in $PAQH_2$ (II). The exergonicity of the porphyrin S_1 state oxidation is sufficiently large (~0.49 eV) to promote rapid reaction.[3a] Nevertheless, the rate constant (4.1×10^8 s^{-1}) for this electron transfer is substantially smaller than those observed for other porphyrin-quinone molecules that possess similar reaction exergonicities and linkages between the porphyrin and quinone. For example, Gust et al.[33] have shown that the rate constant for oxidation of the porphyrin S_1 state by the attached benzoquinone in III is 9.9×10^9 s^{-1} in CH_2Cl_2. This rate is about 25 times faster than we have found for I.[34]

I and III are isomers with regard to bridging group, so this large difference is surprising. It may be that the positioning of the carbonyl function in III midway in the linkage between P and Q increases the degree of electronic coupling between the π systems of the donor and acceptor through a homoconjugative or superexchange mechanism.[35]

In contrast to III, in which the electron-transfer rate is much faster than in I, the rate in IV is only 1.5×10^7 s^{-1} in CH_2Cl_2.[4c] This is 27 times *slower* than the rate in I. The kinetic measurements for III and IV were carried out in CH_2Cl_2 rather than in benzonitrile. However, k_{et}^S for I is almost the same in these two solvents.[15,16] The edge-to-edge distances in I, III, and IV are all about the same, yet k_{et}^S varies by almost 3 orders of magnitude. If electron transfer occurs through a superexchange mechanism involving the antibonding orbitals of the linkage, the totally saturated linkage in IV should indeed exhibit the slowest rate.

Although the linkage in I is flexible, molecular mechanics calculations indicate that the quinone end group is somewhat constrained in terms of the range of distances between it and the porphyrin. These calculations are not exhaustive, since the XIRIS algorithms seek out only local minima while minimizing the bond-strain energy. Nevertheless, the two conformations depicted in Figure 4 appear to represent extremes with respect to the center-to-center distance between the two moieties, and the difference is only ~1.6 in ~14 Å. Of course, such calculations do not address the dynamics of torsional motion about the linking bridge or the most favorable orientation between the two π-ring systems. These factors may play an important role in determining the rates of electron transfer, especially in simple donor–acceptor molecules in fluid solution.

Irrespective of which mechanism is responsible for the observed differences in electron-transfer rates among the porphyrin–quinone molecules I, III, and IV, it is becoming increasingly clear that the bonds of the spacer are strongly involved in determining electron-transfer rates. What role, if any, the solvent plays in

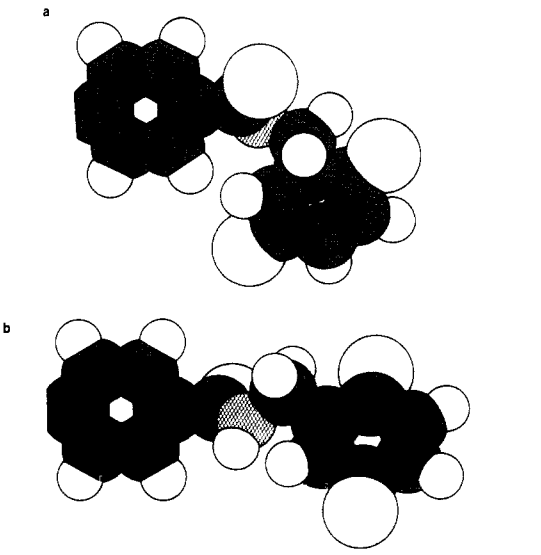

Figure 4. Reproductions of computer-generated models of two conformations of *p*-benzoquinone attached to the para position of a TTP *meso*-phenyl group via an amide bridge (porphyrin ring deleted for clarity). The estimated center-to-center distances between the porphyrin and quinone are 12.7 Å in (a) and 14.3 Å in (b). These structures were generated on a Compaq Model 286 computer with the XIRIS Molecular Modeling System (Version 1.0).

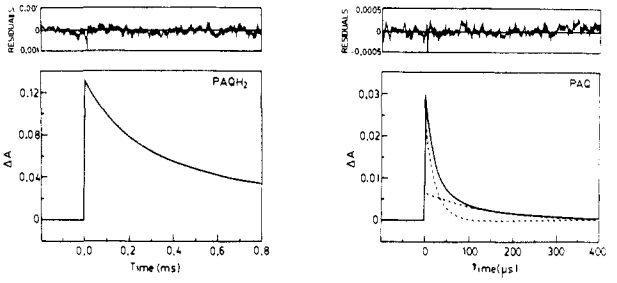

Figure 5. Typical time profiles of porphyrin triplet-state absorbance changes at 455 nm. (a) $PAQH_2$: Observed decay and fit to competing first- and second-order kinetics. Fit parameters for data at representative wavelengths are listed in Table II. (b) PAQ: Observed decay and fit to the sum of two simultaneous exponential components (solid line) and individual components (dashed lines). Table III lists the fit parameters for data taken at several wavelengths. (Data obtained at SERI.)

(27) (a) Gradyushko, A. T.; Sevchenko, A. N.; Solo'vev, K. N.; Tsvirko, M. P. *Photochem. Photobiol.* **1970**, *11*, 387–400. (b) Solo'vev, K.; Tsvirko, M.; Gradyushko, A.; Kozhick, D. *Opt. Spectrosc. (Engl. Transl.)* **1972**, *33*, 480–483.

(28) Gouterman, M. In *The Porphyrins*; Dolphin, D., Ed.; Academic: New York, 1978; Vol. 3, pp 32–33.

(29) Moore, T. A.; Benin, D.; Tom, R. *J. Am. Chem. Soc.* **1982**, *104*, 7356–7357.

(30) Hurley, J. K.; Sinai, N.; Linschitz, H. *Photochem. Photobiol.* **1983**, *38*, 9–14.

(31) Jabben, M.; Garcia, N. A.; Braslavsky, S. E.; Schaffner, K. *Photochem. Photobiol.* **1986**, *43*, 127–131.

(32) Harriman, A.; Hosie, R. J. *J. Photochem.* **1981**, *15*, 163–167.

(33) Gust, D.; Moore, T. A.; Liddell, P. A.; Nemeth, G. A.; Makings, L. R.; Moore, A. L.; Barrett, D.; Pessiki, P. J.; Bensasson, R. V.; Rougée, M.; Chachaty, C.; De Schryver, F. C.; Van der Auweraer, M.; Holzwarth, A. R.; Connolly, J. S. *J. Am. Chem. Soc.* **1987**, *109*, 846–856.

(34) These rates have been confirmed by a mutual exchange of samples with the Arizona State group. There is no significant difference in the electron-transfer rates of III as compared with the molecule that Gust et al. studied[33] with the NH_2 group replaced by a methyl group as in I.

(35) Cave, R. J.; Siders, P.; Marcus, R. A. *J. Phys. Chem.* **1986**, *90*, 1436–1444.

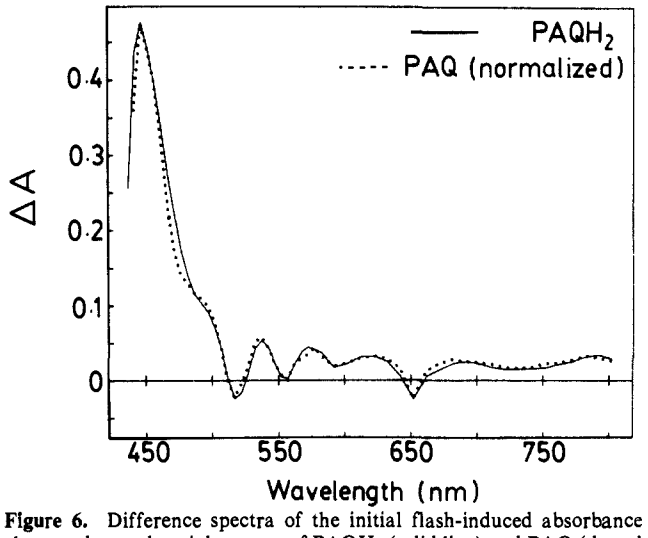

Figure 6. Difference spectra of the initial flash-induced absorbance changes due to the triplet states of $PAQH_2$ (solid line) and PAQ (dotted line) in benzonitrile. The PAQ spectrum has been normalized to the intensity of $PAQH_2$ at the wavelength of the maximum absorbance change. (Data obtained at UWO; these spectra are in excellent agreement with those obtained at SERI.)

determining the distribution of conformations of PAQ, which in turn influence the electron-transfer rate, remains an open question.

4. Triplet-State Photophysics and Photochemistry. Decay profiles of the triplet states of both PAQ and $PAQH_2$ were followed by detecting triplet–triplet (T–T) absorption following ~20 ns laser pulses. Typical kinetic traces are shown in Figure 5, and the corresponding absorbance difference spectra of PAQ and $PAQH_2$ are shown in Figure 6. The difference spectrum of $PAQH_2$ is, as expected, very similar to the T–T difference spectrum of TPP,[25] with a strong absorption ($\lambda_{max} \cong 448$ nm) to the red of the ground-state Soret band and a broad, weak absorption extending to 830 nm (wavelength limit of the SERI monitoring system) with a weak maximum at ~790 nm.

Initially, we thought that the faster absorbance decay in the PAQ samples (Figure 5b) might arise from the presence of a significant concentration of $P^{\bullet+}AQ^{\bullet-}$; however, a careful analysis of the time-resolved difference spectra (vide infra) shows that PAQ exhibits virtually the same difference spectrum as that of $PAQH_2$ (see Figure 6). We therefore conclude that in PAQ we are observing enhanced decay of ^3PAQ.

The decay of the $^3PAQH_2$ absorption at 455 nm (Figure 5a) is described by competing first- and second-order kinetics, as outlined in Scheme I.[25,36,37] The rate of absorbance change is

Scheme I

$$T_1 \xrightarrow{k_1} S_0$$

$$T_1 + T_1 \xrightarrow{k_2} 2S_0$$

$$T_1 + S_0 \xrightarrow{k_3} 2S_0$$

thus given by eq 2 where $\Delta A(t)$ is the absorbance change at time t, C_0 is the total concentration of porphyrin species, $\Delta\epsilon$ is the difference between the ground- and triplet-state extinction coefficients, and l is the path length (in our case 1.00 cm). The

$$-\frac{d\Delta A(t)}{dt} = (k_1 + k_3C_0)\Delta A(t) + \frac{(k_2 - k_3)}{\Delta\epsilon l}[\Delta A(t)]^2 \quad (2)$$

absorbance decay profile of $^3PAQH_2$ in Figure 5a can be fit to the integrated form of this equation[37c] to obtain values for $k_1' = (k_1 + k_3C_0)$, $k_2'/\Delta\epsilon l = (k_2 - k_3)/\Delta\epsilon l$, and ΔA_0, the initial absorption change extrapolated to the time of the laser pulse. Both k_1' and the product $(k_2'/\Delta\epsilon l)(\Delta A_0) = k_2'[T]_0$ (where $[T]_0$ is the concentration of triplet states at time zero) must be independent of the monitoring wavelength if the absorbance change arises from only one transient species.[37] The data presented in Table II indicate that $k_2'[T]_0$ is wavelength independent (within experimental error), while k_1' shows some variation with detection wavelength. However, since the decay is dominated by the second-order term, fluctuations in k_1' are to be expected except for noise-free data.

Table II. Triplet-State Decay Kinetics in $PAQH_2$[a]

A_{532}[b]	λ[c]/nm	k_1'[d] s^{-1}	$[k_2'/\Delta\epsilon l]$[e]/ 10^4 s^{-1}	ΔA_0[f]	$k_2'[T]_0$/ 10^4 s^{-1}
0.042_6	325	605	6.19	0.070	0.432
0.042_6	400	1270	−11.7	−0.030	0.354
0.042_6	430	716	−0.957	−0.334	0.320
0.042_6	440	38	3.38	0.135	0.457
0.042_6	450	168	2.28[g]	0.190	0.432
0.042_6	455	225	2.38	0.134	0.318
0.042_6	475	478	4.49	0.087	0.390
0.200	780	137	30.1	0.038	1.15
0.200	790	514	27.5	0.040	1.11
0.200	800	463	30.0	0.036	1.09

[a] Decay profiles were recorded over 800 μs and analyzed over 700 μs (see Figure 5a). k_1', k_2', ΔA_0, and $[T]_0$ are defined in the text. (Data obtained at SERI.) [b] Ground-state absorbance at the excitation wavelength (532 nm). [c] Monitoring wavelength. [d] Includes a contribution for k_3C_0 (eq 2). [e] ±10%; l = 1.00 cm. [f] ±10%; time zero ≅ 1.95 μs after laser flash. [g] If $\Delta\epsilon \simeq 5 \times 10^4$ cm^{-1},[26] then $k_2' \simeq 1.1 \times 10^9$ s^{-1}, which is in good agreement with the corresponding values for ^3TPP.[25]

Table III. Triplet-State Decay Kinetics in PAQ[a]

λ[b]/nm	A_S^0[c]/10^{-2}	$k_S/10^4$ s^{-1}	A_L^0[c]/10^{-2}	$k_L/10^3$ s^{-1}
440	6.30	5.08	1.16	5.50
445	8.97	4.75	2.13	6.30
450	9.15	4.68	2.40	6.32
455	9.31	4.63	2.34	6.21
460	8.21	4.61	2.09	6.37
470	5.34	4.45	1.49	6.10
480	3.57	4.49	1.04	5.80
490	2.35	4.50	0.76	6.07
500	1.89	4.55	0.61	5.77
790[d]	1.02	5.48	0.34	8.51

[a] The decay kinetics were fit to a sum of two exponential components (see text). A_S^0 and k_S are the preexponential factor and rate constant for the short-lived decay, while A_L^0 and k_L refer to the long-lived component. Except as noted, the decay profiles were recorded over 400 μs and analyzed over 350 μs (see Figure 5b). (Data obtained at SERI.) [b] Monitoring wavelength. [c] Fits extrapolated to the digitizer address of the laser flash (500 μs full scale ≅ 0.977 μs/address); amplitudes not corrected for PAQ photoreduction. Standard error ±10%. [d] Decay kinetics measured over 160 μs; analysis interval was 140 μs.

The decay kinetics of ^3PAQ at 455 nm (Figure 5b) are much faster than those of $^3PAQH_2$. Also ΔA_0 is much smaller (for samples having equal absorbance at the excitation wavelength); this lower triplet yield is qualitatively consistent with the observed quenching of $^1P^*AQ$ (see also Table I).

The decay of ^3PAQ cannot be fit to competing first- and second-order kinetics (Scheme I); thus, enhanced second-order processes do not account for the rapid depletion of ^3PAQ. Instead, the decay profile of ^3PAQ is best described by the sum of two independent exponential decay components as in eq 3 where A_S^0,

$$A(t) = A_S^0 \exp[-k_S t] + A_L^0 \exp[-k_L t] \quad (3)$$

A_L^0 and k_S, k_L are the initial amplitudes and rate constants, respectively, for the short- and long-lived components. The fact that the rate constants are essentially independent of monitoring wavelength (Table III) lends support to this interpretation, since any appreciable second-order component would impart a distinct wavelength dependence on the analyses.[37c]

We assign the short-lived component (k_S) to unimolecular decay of ^3PAQ. The value of k_S, estimated from fits at several wave-

(36) Linschitz, H.; Steel, C.; Bell, J. A. *J. Phys. Chem.* **1962**, *66*, 2574–2576.
(37) (a) Linschitz, H.; Sarkanen, K. *J. Am. Chem. Soc.* **1958**, *80*, 4826–4832. (b) Connolly, J. S.; Gorman, D. S.; Seely, G. R. *Ann. N.Y. Acad. Sci.* **1973**, *206*, 649–669. (c) Gorman, D. S.; Connolly, J. S. *Int. J. Chem. Kinet.* **1973**, V, 977–989.

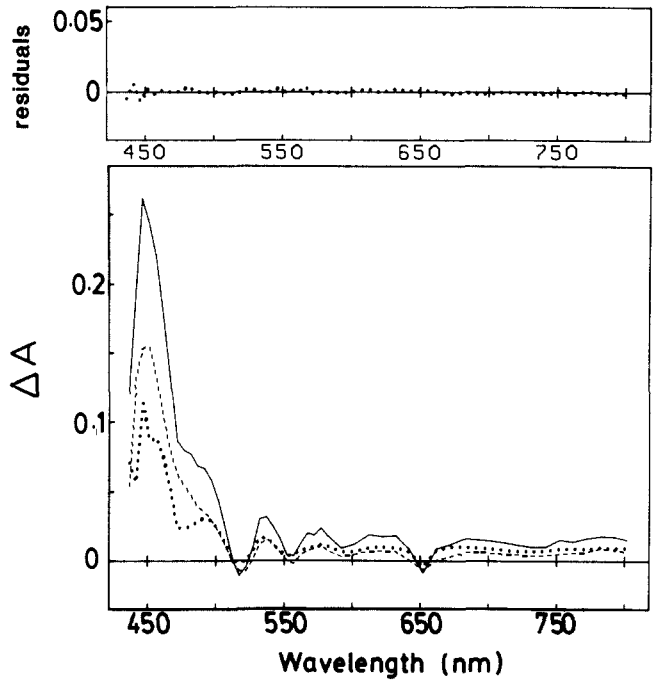

Figure 7. Difference spectra of the two components observed in the decay of ^{3}PAQ: solid line, total ΔA_0 (observed at 0.98 μs after the laser flash); dashed line, amplitudes of short-lived component (A_S^0); dotted line, amplitudes of long-lived component (A_L^0). These spectra were generated by fitting the observed decay profiles to eq 3 with $k_S = 4.6 \times 10^4$ s^{-1} and $k_L = 6.0 \times 10^3$ s^{-1} at all wavelengths. Residuals = $\Delta A_0 - (A_S^0 + A_L^0)$. (Data obtained at UWO; results are in excellent agreement with those obtained at SERI.)

lengths, is 4.6 (±0.2) × 10^4 s^{-1} as compared to ~500 s^{-1} for the first-order component in the decay of ^{3}PAQH$_2$ (Table II). If we make the reasonable assumption that oxidation of the attached hydroquinone of PAQH$_2$ has little effect on the rates of phosphorescence or intersystem crossing to the ground state, it is clear that a new decay pathway overwhelms the other unimolecular deactivation processes in ^{3}PAQ. We assume that this new decay pathway is electron transfer from ^{3}PAQ to the triplet radical-ion-pair state ^{3}(P$^{\bullet+}$AQ$^{\bullet-}$); thus, we identify k_S with k_{et}^T in Figure 1.

The long-lived component (k_L) is ascribed primarily to ^{3}PAQH$_2$, which is present due to incomplete oxidation during sample preparation and to in situ reduction of PAQ during the laser flash experiments (see the Experimental Section). The disparity between k_1' (Table II) and k_L (Table III) is probably due to contributions by T–T annihilation, which should not be neglected but which the fitting routine[37c] cannot resolve when searching for the best fit of the data to two first-order terms (already a four-parameter fit).[21a]

Figure 7 shows the spectral dependence of the absorbance amplitudes of the short- and long-lived components in the relaxation of ^{3}PAQ. These difference spectra were generated by fixing the rate constants and allowing the amplitudes to vary while the observed profiles were fit to the sum of two simultaneous exponentials.[21a] For both components the positions of the absorption maxima and isosbestic points are very similar to those in the overall difference spectrum and are likewise similar to the T–T absorption spectrum of PAQH$_2$ (Figure 6). This supports our conclusion that both the fast and slow processes arise from triplet porphyrin decay and not from some other transient species such as a radical ion pair or a triplet exciplex.[38]

We have also examined transient absorption changes for ^{3}PAQ in several other solvents. In *n*-butyl alcohol the kinetic and spectral profiles are similar to those seen in benzonitrile; the yield of ^{3}PAQ is lower than that of ^{3}PAQH$_2$ in solutions of the same absorbance

Table IV. Comparison of Calculated and Experimental Ratios of Electron-Transfer Rate Constants in PAQ in Benzonitrile.

rate constant ratio	$\Delta G_a°$[a]	$\Delta G_b°$	exptl ratio	calcd ratio[b]
k_{et}^S/k_r^S	−0.49	−1.41	2.6	2.8
k_{et}^S/k_{et}^T	−0.49	−0.02	8.9×10^3	7.1×10^2

[a] Estimated from measured reduction potentials with a coulombic work term correction using the bulk dielectric constant. [b] Calculated by eq 5 with $\lambda = 0.90$ eV.[23]

at the laser wavelength, and the decay of ^{3}PAQ is much faster than that of ^{3}PAQH$_2$. Fits of the ^{3}PAQ decay to the sum of two exponentials yield the quenching rate constant $k_{et}^T = 3.3$ (±0.3) × 10^5 s^{-1}, which is a factor of nearly 7 times higher than in benzonitrile. However, in dioxane, butyronitrile, acetonitrile, and ethyl acetate, we observed only slightly lower triplet yields of PAQ relative to PAQH$_2$, which is consistent with the marginal fluorescence quenching[15] observed in these solvents. Moreover, the decay kinetics of ^{3}PAQ and ^{3}PAQH$_2$ are very similar to each other, indicating that, like the singlet state, very little intramolecular triplet quenching occurs in these solvents.

We have not been able to detect directly the product of quenched ^{3}PAQ. However, we have indirect evidence that the mechanism involves electron transfer. Specifically, the rate constant k_{et}^T is in reasonable agreement with the that predicted by Marcus theory (see next section).

From studies of magnetic field effects on excited-state yields in other systems involving radical pairs,[39] we expect that the electron spins in the initially formed ^{3}(P$^{\bullet+}$AQ$^{\bullet-}$) will rephase to a 3:1 statistical mixture of triplet and singlet spin states within ~20 ns. Accordingly, we suggest that the ^{3}(P$^{\bullet+}$AQ$^{\bullet-}$) state decays to the ground state via the short lived ^{1}(P$^{\bullet+}$AQ$^{\bullet-}$) state on this time scale. In any case the *maximum* concentration of ^{3}(P$^{\bullet+}$AQ$^{\bullet-}$) would be too low ($\leq 10^{-9}$ M) and its lifetime too short to be detected by optical techniques.

5. Marcus Interpretation of Electron-Transfer Rate Constants. In the context of the semiclassical Marcus theory, k_{et} is given by[13c] eq 4 where H_{ps} is an electronic coupling matrix element, λ is the reorganization energy, and $\Delta G°$ is the standard Gibbs energy change in the electron-transfer reaction. For a given solvent

$$k_{et} = \frac{2\pi}{\hbar} \frac{H_{ps}^2}{(4\pi\lambda kT)^{1/2}} \exp\left[-\frac{(\lambda + \Delta G°)^2}{(4\lambda kT)}\right] \quad (4)$$

(constant λ) the ratio of two electron-transfer rate constants for processes a and b of different exergonicities $\Delta G_a°$ and $\Delta G_b°$ is given by eq 5. Table IV displays a comparison of the predicted

$$\frac{k_{et}^a}{k_{et}^b} = \frac{[H_{ps}^a]^2}{[H_{ps}^b]^2} \exp\left[-\frac{[2\lambda(\Delta G_a° - \Delta G_b°) + (\Delta G_a°)^2 - (\Delta G_b°)^2]}{4\lambda kT}\right] \quad (5)$$

and experimental ratios for k_{et}^S vs k_{et}^r and k_{et}^S vs k_{et}^T. If we assume that $H_{ps}^a = H_{ps}^b$, the agreement is excellent for k_{et}^S/k_r^S and within a factor of 10 for k_{et}^S/k_{et}^T. It may be that electron transfer within the triplet manifold involves different matrix elements in H_{ps}. Nevertheless, this analysis shows that the Marcus theory works well in explaining the electron-transfer rate constants in PAQ. In particular, the back-electron-transfer process ($\Delta G°$ = −1.41 eV) is in the "inverted region" and is thus expected to be slower than the forward rate, in agreement with the observation that $k_r^S < k_{et}^S$. The excellent agreement between the experimental and calculated ratios may be fortuitous, as quantum mechanical models[40] of the inverted region predict that this ratio should be

(38) Roy, J. K.; Carroll, F. A.; Whitten, D. G. *J. Am. Chem. Soc.* **1974**, *96*, 6349–6355.

(39) Wasielewski, M. R.; Norris, J. R.; Bowman, M. K. *Faraday Discuss. Chem. Soc.* **1984**, *78*, 279–288.

(40) Siders, P.; Marcus, R. A. *J. Am. Chem. Soc.* **1981**, *103*, 748–752.

Table V. Summary of the PAQ Rate Constants in Figure 1

rate constant	value/s^{-1}	rate constant	value/s^{-1}
k_f	1.2×10^7	k_r^S	$1.6 (\pm 0.2) \times 10^8$
k_{ic}	1.6×10^7	k_T	$2.1 (\pm 0.2) \times 10^2$ [a]
k_{isc}	5.7×10^7	$k_{et}^T \cong k_{-et}^T$	$4.6 (\pm 0.2) \times 10^4$
k_{et}^S	$4.1 (\pm 0.3) \times 10^8$	$k_{31} \cong k_{13}$	$\sim 5 \times 10^7$ [b]

[a] Same as k_1 in Scheme I; value from ref 21a. [b] Estimated.[39]

somewhat smaller than that given by eq 5.

Conclusions

Both the S_1 and T_1 states of the porphyrin chromophore in PAQ are quenched relative to the corresponding states in $PAQH_2$. We have demonstrated conclusively that $^1P^*AQ$ is quenched by electron transfer, leading primarily to formation of $P^{\bullet+}AQ^{\bullet-}$. This is one of the first examples[5c] of *direct* optical evidence for photoinduced charge separation from the S_1 state of a simple tetraarylporphine attached to a quinone by a flexible linkage. Our results thus verify the earlier assignments made by several groups[1-7,15,17,33] that electron transfer is responsible for the observed fluorescence quenching in a variety of flexibly linked porphyrin-quinone molecules. Furthermore, comparison of the electron-transfer rate constants in PAQ with respect to other porphyrin-quinone systems shows that the rates are strongly affected by the nature of the linkage between the two moieties and that electron transfer involves through-bond interactions in the covalent bridge.[3c,41]

The T_1 state of the porphyrin in PAQ is also quenched, probably by electron transfer, although the presumed $^3(P^{\bullet+}AQ^{\bullet-})$ product was not observed. We attribute this to the inherent rates in this molecular model system and not to instrument limitations.

We have examined the PAQ porphyrin-quinone system, and its hydroquinone analogue, by steady-state absorption and emission spectroscopy and by laser flash-induced kinetics on the picosecond to millisecond time scale. Thus, we have been able to evaluate rate constants for all of the steps indicated in Figure 1. These values are listed in Table V. The ratios of electron-transfer rate constants are in reasonable agreement with those predicted from Marcus theory.

Acknowledgment. This work was supported by a Strategic Grant in Energy and Operating Grants to J.R.B. and A.C.W. from the Natural Sciences and Engineering Research Council of Canada and by funding from the Division of Chemical Sciences, Office of Basic Energy Sciences, U.S. Department of Energy to J.S.C. (Contract No. DE-AC02-83CH10093) and M.R.W. (Contract No. W-31-109-Eng-38). J.A.S. acknowledges the support of an Ontario Graduate Scholarship from the Ontario Ministry of Colleges and Universities. We are grateful to Dr. Mary Archer for helpful discussions.

Registry No. PAQ, 112712-62-6; $PAQH_2$, 112712-63-7.

(41) Heitele, H.; Michel-Beyerle, M. E. *J. Am. Chem. Soc.* **1985**, *107*, 8286-8288.

Biosynthesis of Triterpenes, Ursolic Acid, and Oleanolic Acid in Tissue Cultures of *Rabdosia japonica* Hara† Fed [5-$^{13}C^2H_2$]Mevalonolactone and [2-$^{13}C^2H_3$]Acetate

Shujiro Seo,*‡ Yohko Yoshimura,‡ Atsuko Uomori,‡ Ken'ichi Takeda,‡ Haruo Seto,§ Yutaka Ebizuka,∥ and Ushio Sankawa∥

Contribution from the Shionogi Research Laboratories, Shionogi & Co., Ltd., Fukushima-ku, Osaka 553, Japan, the Institute of Applied Microbiology, University of Tokyo, Yayoi, Bunkyo-ku, Tokyo 113, Japan, and the Faculty of Pharmaceutical Science, University of Tokyo, Hongo, Bunkyo-ku, Tokyo 113, Japan. *Received March 11, 1987*

Abstract: [5-$^{13}C^2H_2$]Mevalonolactone and sodium [2-$^{13}C^2H_3$]acetate were fed to suspension cultures of *Rabdosia japonica* Hara. The ^{13}C-^2H labeling patterns analyzed by ^{13}C-{^1H}{^2H} NMR spectroscopy for methyl ursolate (**13**) and methyl oleanolate (**15**) give the biosynthetic information for all the hydrogen atoms composing mevalonic acid incorporated into these two triterpenes. The combination of the labeling patterns on C(11)-C(12) in one molecule of ursolate from [5-$^{13}C^2H_2$]MVA being $^{13}C(11)^2H_2$-$^{13}C(12)^2H$ and $^{13}C(11)^2H^1H$-$^{13}C(12)^2H$ differ from those of oleanolate [$^{13}C(11)^2H_2$-$^{13}C(12)^1H$ and $^{13}C(11)^2H^1H$-$^{13}C(12)^2H$]. This indicates that ursolic acid (**12**) and oleanolic acid (**14**) are formed from both oxidosqualenes **8** and **9** and the 12(13) double bond of **12** is formed by elimination of the 12-*pro-R* hydrogen atom of **10** and **11** in a cis mode. Three signals shifted by β-deuterium atoms verify the 1,2-hydride shifts (20-H from C-19,19-H from C-18, and 18-H from C-13) in the biosynthesis of ursolic acid (**12**) from [2-$^{13}C^2H_3$]acetate. Two β-deuterium-shifted signals confirm the 1,2-hydride shifts (19-H from C-18 and 18-H from C-13) in the biosynthesis of oleanolic acid (**14**) from [2-$^{13}C^2H_3$]acetate.

Squalene is an achiral molecule formed by tail-to-tail coupling of two molecules of farnesyl pyrophosphate (FPP) starting from acetic acid via mevalonic acid (MVA), isopentenyl pyrophosphate (IPP), γ,γ-dimethylallyl pyrophosphate (DMAPP), and geranyl pyrophosphate.[1] The 12-*pro-R* hydrogen atom of squalene is derived from the 4-*pro-S* hydrogen atom (H*) of NADPH, because (1*R*,2*R*,3*R*)-presqualene, which is formed with loss of the 1-*pro-S* hydrogen atom of one of the two FPP, is reduced by

Scheme I

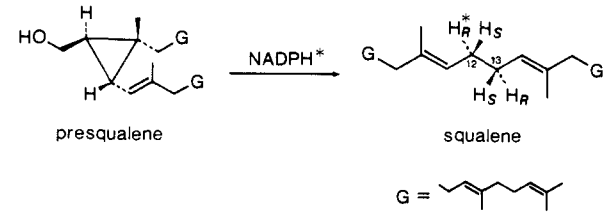

NADPH to give squalene (Scheme I).[2] The mechanism of the reductive ring-opening reaction has been studied.[3] Due to the

† *Rabdosia japonica* Hara was formerly called *Isodon japonicus* Hara.
‡ Shionogi Research Laboratories, Shionogi & Co., Ltd.
§ Institute of Applied Microbiology, University of Tokyo.
∥ Faculty of Pharmaceutical Science, University of Tokyo.

0002-7863/88/1510-1740$01.50/0